

<https://doi.org/10.1038/s41538-025-00476-x>

Integrated transcriptomic analysis unveils molecular mechanisms regulating meat quality in newly improved black goat breeds

Check for updates

Yong Long^{1,2}, Naifeng Zhang³, Yanliang Bi³, Tao Ma³, Pramote Paengkoum², Wen Xiao⁴, Yanpin Zhao⁴, Chao Yuan⁴, Defeng Wang⁴, Yang Yang⁴, Chaozhi Su⁴ & Yong Han^{1,4}✉

This study aimed to integrate transcriptomes to reveal the regulatory molecular mechanisms of meat quality in different black goat breeds. A comparison of Guizhou Black Goats (GBG♂, $n = 7$), Black Nubian Goats (NBG♂, $n = 7$), and their F1 hybrids (FBG♂, GB♀ × NB♂, $n = 7$) revealed that the FBG demonstrated notable improvements in meat quality parameters, muscle fiber traits, fatty acid and amino acid compositions, mineral content, intramuscular fat (IMF), and inosine monophosphate (IMP) levels. Moreover, transcriptome analysis identified 119, 77, and 82 differentially expressed genes (DEGs) in the GBG vs NBG, FBG vs GBG, and FBG vs NBG comparisons, respectively. Among these, 111, 74, and 82 DEGs were associated with IMF deposition, and 61, 34, and 32 DEGs were linked to IMP deposition, respectively. Of particular note, the analysis pinpointed key genes related to IMF (*PFKM* and *FZD4*) and IMP (*AMPD3*, *ENPP1*, *ENTPD1*, *ENTPD8*, and *PRPS2*), laying a solid data groundwork for future research aimed at enhancing the meat quality of black goats.

Goats (*Capra hircus*) are among the earliest domesticated animals, with a history exceeding 10,000 years. China currently maintains around 60 indigenous breeds, each with unique characteristics¹. Guizhou black goat (GBG) is one of the three typical goat breeds in Guizhou. It is a Chinese national geographical indication of specialty agricultural products and has been included in the list of local fine breeds protected in Guizhou province². The unique ecological environment of the karst landscape and harsh natural selection have made GBG cold-resistant and tolerant to roughage, with strong walking ability, strong stress resistance, and excellent survival skills. Additionally, GBG is renowned for its tender meat, low cholesterol, lower odor, and good gregariousness. So far, the annual stock of GBG is ~500,000^{3,4}. However, GBG faces issues such as small size, slow growth, high fattening costs, and low slaughter rates, which significantly hinder the high-quality development of the GBG industry⁵. Therefore, the question of how to carry out GBG breeding and improvement to enhance growth performance, meat quality, and economic returns remains one of our most pressing concerns.

At present, the primary approach to improving goat breeding in China involves introducing excellent foreign breeds and hybridizing them with

local breeds, followed by selection and breeding to ultimately cultivate new meat-producing goat breeds with superior performance⁶. In an effort to improve and breed GBG, it was concluded by Min et al.⁷ that a high-quality hybrid goat breed (BKF4) was developed through four generations of progressive crossbreeding between GBG and South African Kalahari goats (SKG). The BKF4 exhibited higher lambing rates, daily weight gains, adult weights, and slaughter rates than GBG. However, the overall meat quality of BKF4 was intermediate between that of SK and GB. Moreover, BKF4 has greatly improved the production efficiency, tenderness, juiciness, and chemical composition of the meat. The amino acid and fatty acid composition were more similar to those of SK⁷. However, the excessive focus on hybridization in early breeding efforts, coupled with the neglect of selective breeding, led to significant issues of disordered hybridization and even posed a threat to the conservation of local genetic resources. In response to these issues, Guizhou has recently introduced the excellent Nubian goat breed, known for its good meat production, fast growth, and large size. As a result, hybridization using Nubian goats (NBG) as sires and GBG as dams has proven to be an effective method for improving the meat production, daily weight gain, reproductive rate, and growth rate of GBG^{2,4}.

¹Guizhou University of Traditional Chinese Medicine, Guiyang, China. ²School of Animal Technology and Innovation, Institute of Agricultural Technology, Suranaree University of Technology, Nakhon Ratchasima, Thailand. ³Institute of Feed Research of Chinese Academy of Agricultural Science, Beijing, China. ⁴Institute of Animal Husbandry and Veterinary Sciences, Guizhou Academy of Agricultural Sciences, Guiyang, China. ✉e-mail: Yonghan978@outlook.com

Over the years, the hybridization and improvement of NBG and GBG have yielded positive results in body size, growth performance, and other traits. However, there are few reports on the tenderness and flavor of GBG meat after hybridization, and opinions differ on the mechanisms by which hybridization affects meat quality. The question of whether hybridizing GBG and NBG can improve the meat quality of the new generation of GBG is something we are eager to answer. We hypothesize that hybridization may influence meat quality to varying degrees by regulating the expression of genes involved in multiple pathways related to GBG meat tenderness and flavor. Therefore, this study focused on GBG, NBG, and their first-generation hybrid black goat (FBG) as research subjects, conducting intensive fattening and comparing the differences in nutritional components, intramuscular fat (IMF), inosine monophosphate (IMP), amino acids, fatty acids, trace elements, and muscle fiber characteristics of the *Longissimus thoracis et lumborum* (LTL). Additionally, we conducted transcriptome sequencing analysis on the *LTL* to explore the expression and mechanism of candidate genes related to IMF and IMP, key indicators for evaluating meat quality. The primary objective is to provide a more comprehensive and valuable data foundation that supports the improvement of meat quality in the FBG (Guixi black goat).

Results

Differences in meat quality parameters of different black goat breeds

The pH_{45min} values of FBG and NBG groups were significantly higher ($P < 0.05$) than those of the GBG group. However, the a*, L*, and b* values of the GBG group were significantly higher ($P < 0.01$) than the NBG group, while the a*, L*, and b* values of the FBG group were between the GBG and NBG groups. Moreover, the Warner-Bratzler shear force (WBSF) of the FBG group was significantly lower ($P < 0.05$) than that of the GBG group and showed no statistical significance ($P > 0.05$) with the NBG group. Interestingly, the cooking loss of the GBG group was significantly higher ($P < 0.05$) than that of the other two groups. (Table 1).

Differences in nutritional and mineral composition of different black goat breeds

The content of Ash in the GBG group was significantly higher ($P < 0.05$) than in the NBG group. In the analysis of mineral composition (Table 2), the content of Fe in the GBG group was significantly higher ($P < 0.01$) than in the other two groups. In comparison, the Zn content in the GBG group was significantly higher ($P < 0.01$) than that in the NBG group. Furthermore, the content of Mn in the NBG group was significantly higher ($P < 0.01$) than

that in the GBG group. Notably, the Cu content in the NBG group was significantly higher ($P < 0.05$) than in the other two groups.

Differences in fiber properties and IMF parameters of different black goat breeds

The muscle fiber parameters are shown in Table 3 and Fig. 1A. It could be concluded that the muscle fiber number in the NBG and FBG groups was significantly higher ($P < 0.01$) than that of the GBG group. Moreover, the total muscle fiber area of the FBG group was significantly higher ($P < 0.01$) than that of the GBG and NBG groups. Interestingly, the muscle fiber diameter in the GBG group was significantly higher ($P < 0.05$) than that in the NBG and FBG groups. Among intramuscular fat parameters, the IMF area, MT area, and IMF/MT ratio were significantly higher ($P < 0.01$) in the

Table 2 | Differences in the nutritional mineral composition of LTL in different black goat breeds

Items	Groups			SEM	P value
	GBG	NBG	FBG		
Nutritional composition, %					
Moisture content	68.14	71.23	70.23	1.23	0.572
CP	20.15	18.78	19.27	0.35	0.315
Ash	4.24 ^a	3.62 ^b	3.92 ^{a,b}	0.16	0.017
Mineral composition, mg/kg					
Fe	75.40 ^a	52.22 ^c	60.87 ^b	3.39	<0.01
Mn	0.99 ^b	1.49 ^a	1.61 ^a	0.10	<0.01
Cu	2.98 ^b	4.24 ^a	3.32 ^b	0.23	0.027
Zn	144.23 ^a	126.3- 1 ^b	145.71 ^a	3.47	<0.01
Se	0.10	0.11	0.12	0.00	0.149

Different letters in the same row (e.g., a, b and c) indicate significant ($P < 0.05$) or extremely significant ($P < 0.01$) differences. Please refer to the *p* values provided in each table for detailed information. SEM, standard error of the mean.

Table 3 | Differences in LTL muscle fiber and IMF parameters among different black goat breeds (Observed at 200 times the field of view)

Items	Groups			SEM	P value
	GBG	NBG	FBG		
Muscle fiber parameters					
Muscle fiber number	155.1- 1 ^b	200.00 ^a	212.22 ^a	11.- 14	<0.01
Muscle fiber diameter (mm)	0.08 ^a	0.06 ^b	0.06 ^b	0.00	0.012
Total muscle fiber area (mm ²)	0.35 ^b	0.33 ^b	0.40 ^a	0.01	<0.01
Muscle fiber density (number/mm ²)	464.99	600.91	548.08	35.- 28	0.295
Intramuscular fat parameters					
IMF	5.67 ^c	9.67 ^a	7.60 ^b	0.59	<0.01
IMF area (mm ²)	7.64 ^c	32.80 ^a	16.77 ^b	1.78	<0.01
MT area (cm ²)	23.38 ^b	37.27 ^a	32.39 ^a	2.19	<0.01
IMF/MT (%)	0.32 ^b	0.88 ^a	0.53 ^b	0.09	<0.01

IMF intramuscular fat, MT muscle tissue, IMF/MT intramuscular fat/muscle tissue.

Different letters in the same row (e.g., a, b and c) indicate significant ($P < 0.05$) or extremely significant ($P < 0.01$) differences. Please refer to the *p* values provided in each table for detailed information. SEM, standard error of the mean.

Table 1 | Differences in LTL meat quality parameters among different black goat breeds

Items	Groups			SEM	P-value
	GBG	NBG	FBG		
pH _{45min}	5.95 ^b	6.20 ^a	6.20 ^a	0.05	0.036
pH _{24h}	5.80	5.93	5.92	0.04	0.406
ΔpH	0.15	0.27	0.28	0.04	0.388
L*	36.10 ^a	28.34 ^c	31.70 ^b	1.15	<0.01
a*	11.04 ^a	8.32 ^b	11.14 ^a	0.49	<0.01
b*	11.40 ^a	7.62 ^b	9.53 ^{a,b}	0.61	<0.01
WBSF, N	47.02 ^a	44.89 ^{a,b}	41.70 ^b	0.95	0.036
Cooking loss, %	38.35 ^a	34.77 ^b	34.65 ^b	0.76	0.046

ΔpH = pH_{45min} - pH_{24h}; L*, lightness; a*, redness; b*, yellowness; WBSF Warner-Bratzler shear force.

Different letters in the same row (e.g., a, b and c) indicate significant ($P < 0.05$) or extremely significant ($P < 0.01$) differences. Please refer to the *p* values provided in each table for detailed information. SEM, standard error of the mean.

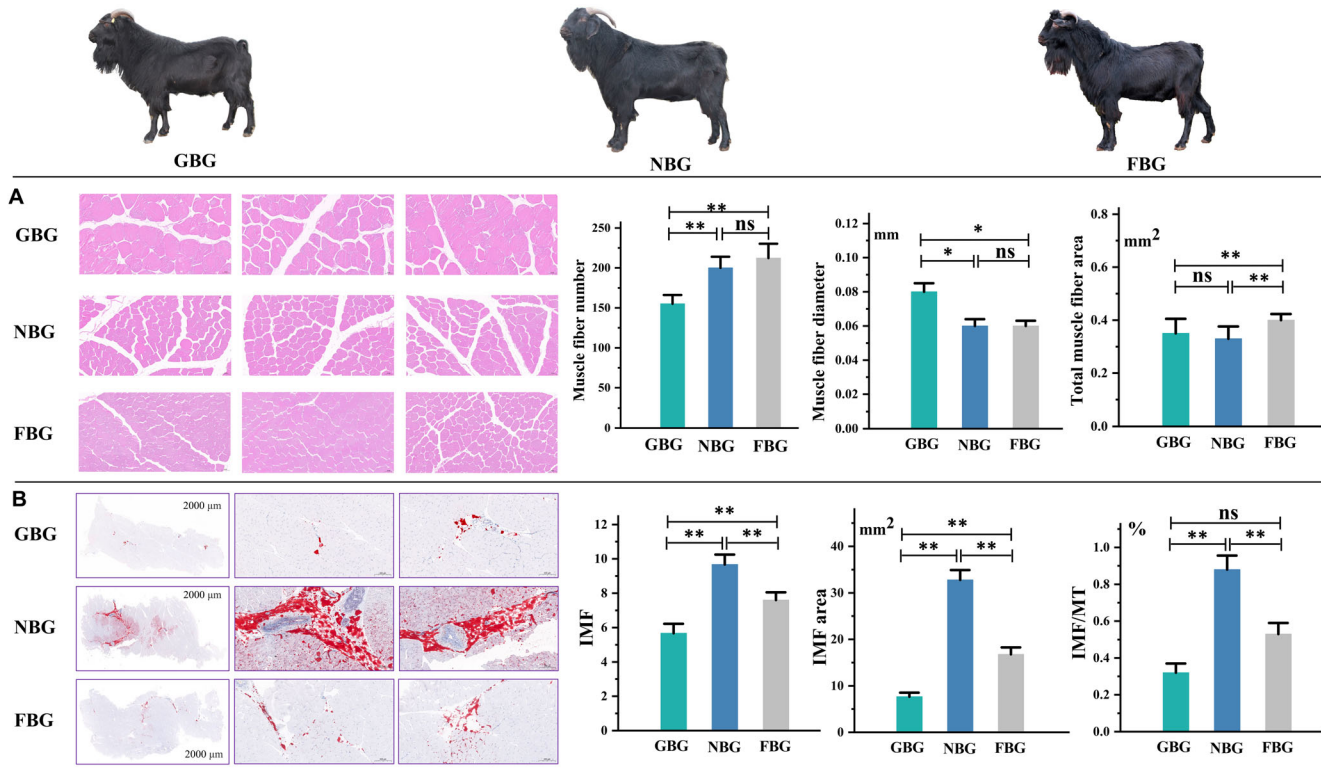


Fig. 1 | Effects of different black goat breeds on muscle fiber and intramuscular fat parameters of *longissimus thoracis et lumborum*. A muscle fiber characteristics analysis; **B** IMF content analysis. * $P < 0.05$; ** $P < 0.01$; ns no statistical significance.

NBG group than in the GBG group, with FBG values falling in between (Table 3, Fig. 1B).

Differences in fatty acid profiles of different black goat breeds

It could be concluded from Table 4 that C10:0 and C12:0 in the GBG and FBG groups were significantly higher ($P < 0.01$) than those in the NBG group. Interestingly, the contents of C16:0, C16:1, C17:1, and C18:0 in FBG *LTL* were significantly increased ($P < 0.01$) by hybridization technology. Similarly, the AI and TI indices of the FBG group were also significantly higher ($P < 0.05$) than those of the GBG group. Notably, compared with the GBG group, the contents of SFA, MUFA, DFA, and UFA in the FBG group were significantly increased ($P < 0.01$). Unexpectedly, the Σ -6 value in the FBG group was significantly higher ($P < 0.01$) than that in the NBG group. The ratio of PUFA/SFA in the GBG group was significantly higher ($P < 0.05$) than that in the FBG group.

Differences in amino acid profile of different black goat breeds

Compared with the GBG group, the hybridization of GBG and NBG significantly increased ($P < 0.05$) the contents of Leu, Phe, and Arg in the muscle. However, the improvement effect of Lys, Met, Ile, and Arg was more obvious ($P < 0.01$). Moreover, the contents of EAA, FAA, and BCAA in the FBG group was significantly higher ($P < 0.05$) than those in the GBG group. Similarly, the TAA and DAA contents in the FBG group were also significantly higher ($P < 0.01$) than those in the GBG group. Finally, the EAA/TAA content in the FBG group was also significantly higher ($P < 0.05$) than that in the GBG group. (Table 5).

Differences in IMP and decomposition products (hypoxanthine, inosine, AMP, and ADP) of different black goat breeds

The contents of IMP and ADP in the NBG group were significantly higher ($P < 0.05$) than those in the GBG group. Furthermore, the Hypoxanthine content in the NBG and GBG groups was significantly higher ($P < 0.05$) than in the FBG group. (Table 6).

Differences in transcriptome analysis of different black goat breeds

Through transcriptome sequencing, a total of 199,271,617 raw reads were obtained from all samples. After the quality check of the raw data, 195,589,610 clean reads were obtained, with GC content ranging from 48.63% to 52.60%, Q20 and Q30 values exceeding 97.24% and 92.56%, respectively, and an error rate of only 0.02–0.03 (Supplementary Table 1). A comparison of clean reads with the transcriptome reference sequence assembled by Trinity revealed that the alignment rate of each sample exceeded 75%, ranging from 76.96% to 78.23% (Supplementary Table 2).

In the Venn diagram (Supplementary Fig. 1), 51794, 54125, and 58512 genes were identified in the GBG, NBG, and FBG groups, respectively. From the cluster heatmap, we observed that among all the genes identified in the three breeds of black goats, many genes exhibited significant differences (Fig. 2A). In addition, Principal component analysis (PCA) (Fig. 2B) showed that the contribution rate of differences between groups was relatively large, indicating that the differences in genes between groups were significant. 1255 unique DEGs were identified in GBG vs NBG. Moreover, 217 DEGs were shared with FBG vs GBG, and 152 DEGs shared with FBG vs NBG were identified in GBG vs NBG. 663 and 640 unique DEGs were identified in FBG vs GBG and FBG vs NBG, respectively (Fig. 2C). Among the DEGs, FBG vs GBG (Supplementary Data 1) had 723 genes that were upregulated and 506 genes that were downregulated. FBG vs NBG (Supplementary Data 2) had 789 genes that were upregulated and 352 genes that were downregulated, GBG vs NBG (Supplementary Data 3) had 1002 genes that were upregulated and 627 genes that were downregulated (Fig. 2D, E).

In Gene Function Classification (Fig. 2F), DEGs were mainly enriched in cellular process and metabolic process at the Biological Process (BP) level; the cellular anatomical entity and intracellular at the Cellular Component (CC) level; and binding and catalytic activity at the Molecular Function (MF) level. In KEGG Classification, DEGs are mainly enriched in branch B, including Protein families: genetic information processing, Protein families: signaling and cellular processes, and Protein families: metabolism (Fig. 2G).

Table 4 | Differences in LTL fatty acid profiles among different black goat breeds (mg/g)

Items	Group				SEM	P value
		GBG	NBG	FBG		
C4:0	1.06	1.03	1.14	0.05	0.721	
C6:0	0.32	0.35	0.27	0.03	0.566	
C8:0	0.63	0.59	0.65	0.04	0.818	
C10:0	0.97 ^a	0.71 ^b	0.97 ^a	0.05	<0.01	
C11:0	0.51	0.50	0.48	0.01	0.609	
C12:0	0.60 ^a	0.44 ^b	0.66 ^a	0.04	<0.01	
C13:0	0.52	0.47	0.48	0.03	0.797	
C14:0	2.03	3.19	3.72	0.54	0.070	
C14:1	0.54	0.53	0.63	0.04	0.516	
C15:0	0.77	0.99	1.10	0.12	0.561	
C15:1	0.32	0.34	0.36	0.02	0.661	
C16:0	24.59 ^c	32.51 ^b	40.74 ^a	2.47	<0.01	
C16:1	1.66 ^b	2.08 ^b	5.13 ^a	0.56	<0.01	
C17:0	1.68 ^b	2.78 ^{a,b}	3.82 ^a	0.37	0.029	
C17:1	2.07 ^b	2.77 ^b	4.52 ^a	0.38	<0.01	
C18:0	34.67 ^b	49.63 ^a	52.60 ^a	2.91	<0.01	
C18:1	7.14 ^b	9.88 ^a	6.34 ^b	0.63	0.020	
C18:2	16.73	18.74	16.96	1.10	0.798	
C18:3 n-3	0.46	0.42	0.44	0.03	0.870	
C20:0	0.56	0.50	0.44	0.03	0.220	
C20:1 n-9	1.02	1.08	1.26	0.06	0.197	
C21:0	0.32	0.37	0.30	0.24	0.535	
C22:1	0.52	0.49	0.41	0.30	0.385	
C22:0	0.64	0.76	0.58	0.06	0.481	
C20:2	0.95	0.91	0.91	0.05	0.956	
C20:3 n-6	0.89	1.01	0.93	0.04	0.589	
C20:4 n-6	5.45 ^{a,b}	4.70 ^b	6.08 ^a	0.18	<0.01	
C23:0	0.23	0.29	0.25	0.01	0.384	
C20:3 n-3	0.38	0.37	0.41	0.02	0.686	
C22:2	0.11	0.09	0.12	0.01	0.312	
C24:0	0.62	0.58	0.57	0.02	0.716	
C24:1	1.05 ^b	1.41 ^a	1.20 ^{a,b}	0.06	<0.01	
SFA	70.75 ^b	95.68 ^a	108.76 ^a	5.96	<0.01	
MUFA	14.32 ^b	18.57 ^{a,b}	19.86 ^a	0.95	<0.01	
PUFA	25.12	26.22	25.84	1.26	0.959	
UFA	39.53 ^b	44.80 ^a	45.70 ^a	1.03	<0.01	
Σ n-3	0.84	0.78	0.84	0.04	0.797	
Σ n-6	6.34 ^{a,b}	5.7 ^b	7.02 ^a	0.28	<0.01	
n-6/n-3	7.64	7.34	8.39	0.33	0.461	
PUFA/SFA	0.36 ^a	0.27 ^{a,b}	0.24 ^b	0.02	0.040	
DFA	74.20 ^b	94.42 ^a	98.30 ^a	4.13	<0.01	
AI	0.85 ^b	1.02 ^{a,b}	1.22 ^a	0.07	0.031	
TI	0.70 ^b	0.91 ^{a,b}	1.05 ^a	0.07	0.032	

SFA saturated fatty acids, MUFA monounsaturated fatty acids, PUFA polyunsaturated fatty acids, UFA unsaturated fatty acids, DFA hypocholesterolemic fatty acids, TI Atherogenicity index, TI Thrombogenic index.

DFA = MUFA + PUFA + C18:0;

TI = $(C12:0 + 4 \times C14:0 + C16:0) / \Sigma UFA$;

TI = $(C14:0 + C16:0 + C18:0) / [(0.5 \times \Sigma MUFA) + (0.5 \times \Sigma n-6) + (3 \times \Sigma n-3) + (\Sigma n-3 / \Sigma n-6)]$.

Different letters in the same row (e.g., a, b and c) indicate significant ($P < 0.05$) or extremely significant ($P < 0.01$) differences. Please refer to the p values provided in each table for detailed information. SEM, standard error of the mean.

Table 5 | Differences in LTL amino acid profiles of different black goat breeds (g/100 g)

Items	Group				SEM	P-value
		GBG	NBG	FBG		
Lys	1.65 ^b	1.78 ^a	1.81 ^a	0.02	<0.01	
Thr	0.83	0.88	0.89	0.01	0.195	
Val	0.84	0.89	0.90	0.01	0.180	
Met	0.13 ^b	0.21 ^a	0.22 ^a	0.01	<0.01	
Ile	0.81 ^b	0.87 ^a	0.88 ^a	0.01	<0.01	
Leu	1.33 ^b	1.45 ^{a,b}	1.47 ^a	0.03	0.025	
Tyr	0.56	0.61	0.62	0.04	0.103	
Phe	0.64 ^b	0.70 ^{a,b}	0.73 ^a	0.02	0.034	
Glu	2.51	2.68	2.75	0.05	0.114	
Asp	1.83	1.91	1.92	0.02	0.263	
Pro	0.63	0.65	0.63	0.01	0.641	
Gly	0.80	0.84	0.81	0.01	0.431	
Ala	0.90 ^b	0.97 ^a	0.94 ^{a,b}	0.01	<0.01	
Arg	1.08 ^b	1.17 ^{a,b}	1.22 ^a	0.03	0.023	
His	0.80	0.83	0.84	0.02	0.554	
Ser	0.71	0.76	0.74	0.01	0.164	
TAA	16.08 ^b	17.19 ^a	17.38 ^a	0.19	<0.01	
NEAA	9.03	9.58	9.63	0.14	0.142	
EAA	7.05 ^b	7.61 ^{a,b}	7.75 ^a	0.14	0.036	
EAA/TAA	0.78 ^b	0.79 ^{a,b}	0.80 ^a	0.01	0.041	
DAA	7.69 ^b	8.21 ^a	8.26 ^a	0.08	<0.01	
LAA	1.79 ^b	2.00 ^a	2.03 ^a	0.05	0.030	
FAA	4.92 ^b	5.29 ^{a,b}	5.45 ^a	0.10	0.029	
SFAA	3.88	4.10	4.01	0.05	0.233	
AFAA	5.14	5.41	5.51	0.08	0.143	
BCAA	2.99 ^b	3.21 ^{a,b}	3.26 ^a	0.06	0.038	

NEAA non-essential amino acids, EAA essential amino acids (Lys, Met, Val, Ile, Leu, Phe, His, and Thr), TAA total amino acids, DAA flavor amino acids (Ala, Gly, Arg, Glu, Asp, and Tyr), LAA limited amino acids (Lys and Met), SFAA sweet flavor amino acids (Ala, Gly, Thr, Ser, and Pro), AFAA acid flavor amino acids (Phe, Asp, Glu, and His), BCAA branched-chain amino acids (Val, Ile, and Leu), FAA functional amino acids (Glu, Leu and Arg).

Different letters in the same row (e.g., a, b) indicate significant ($P < 0.05$) or extremely significant ($P < 0.01$) differences. Please refer to the p values provided in each table for detailed information. SEM, standard error of the mean.

Table 6 | Differences in the composition of LTL umami substances in different black goat breeds (μg/g)

Items				SEM	P-value
	GBG	NBG	FBG		
IMP	2027.92 ^b	2580.29 ^a	2307.09 ^a	90.67	0.028
Hypoxanthine	28.36 ^a	28.34 ^a	22.99 ^b	0.96	0.019
Inosine	6.72	6.56	4.45	0.54	0.153
AMP	109.55	118.27	122.38	4.30	0.525
ADP	281.60 ^b	333.03 ^a	302.15 ^{a,b}	9.24	0.041

AMP Adenosine monophosphate, ADP Adenosine diphosphate.

Different letters in the same row (e.g., a, b) indicate significant ($P < 0.05$) or extremely significant ($P < 0.01$) differences. Please refer to the p values provided in each table for detailed information. SEM, standard error of the mean.

Furthermore, in KOG Function Classification (Fig. 2H), DEGs were mainly distributed in signal transduction mechanisms.

The biological function analysis of target DEGs was performed based on GO functional enrichment (Fig. 3A, B). In GBG vs NBG, DEGs were

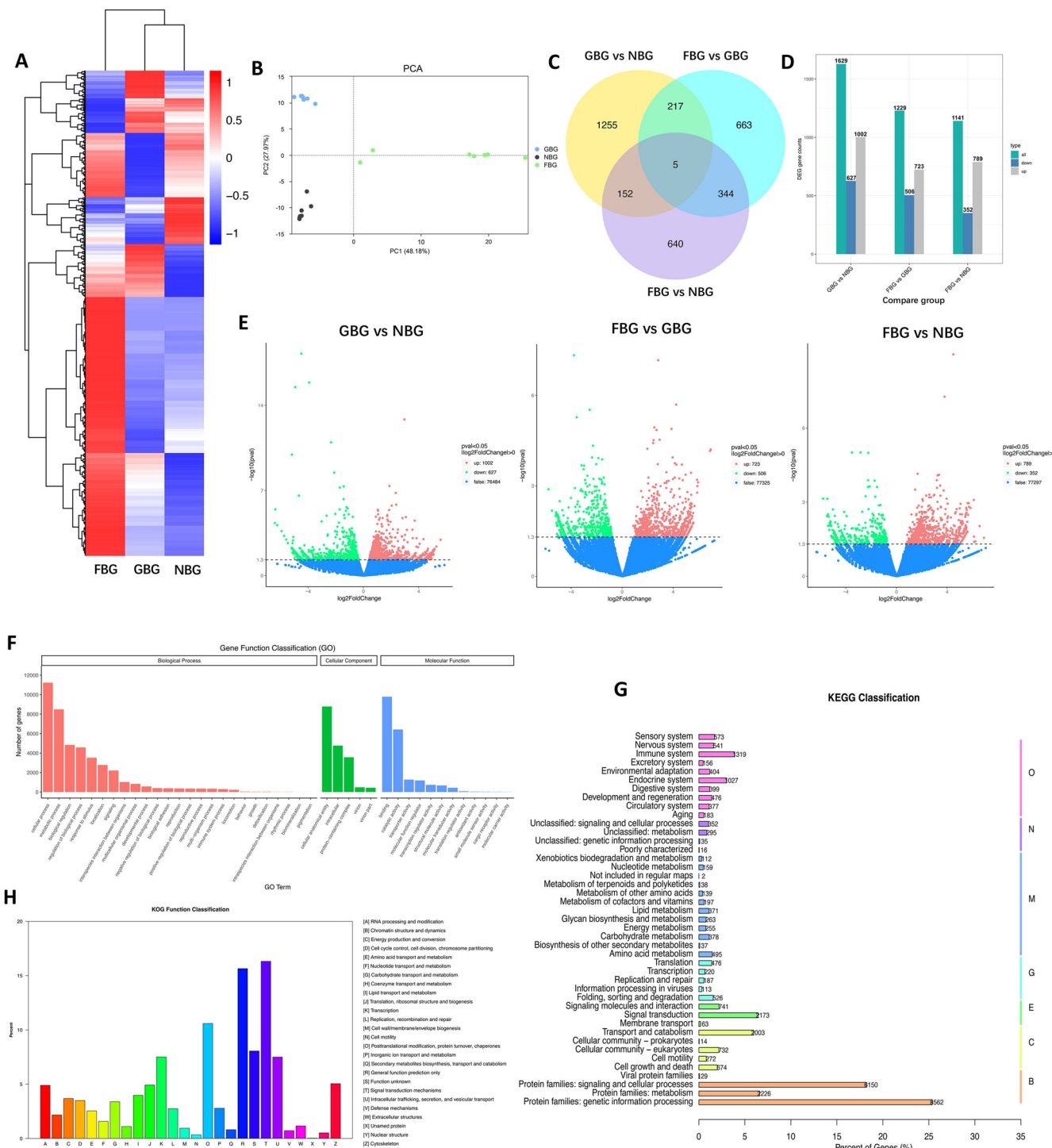


Fig. 2 | Expression profile of DEGs in different breeds of LTL in black goat breeds.
A Cluster heatmap of differentially expressed genes (DEGs); **B** Principal component analysis (PCA) plots; **C** Venn diagram of differentially expressed genes; **D** Statistical bar graph of the number of DEGs in the difference comparison combination; **E** Volcano plot of DEGs; **F** GO annotation classification statistics; **G** KEGG

metabolic pathway classification statistics (O, organismal systems; N, not included in Pathway or Brite; M, metabolism; G, genetic Information processing; E, environmental Information processing; C, cellular processes; B, Brite hierarchies); **H** KOG annotation classification statistics.

highly enriched in the plasma membrane and reproductive process. In FBG vs GBG, DEGs were highly enriched in cell adhesion, signaling, and molecular transducer activity. Notably, the functional enrichment of DEGs was more pronounced in FBG vs NBG, where they were highly enriched in signaling, programmed cell death, and cell adhesion. Additionally, we performed a more detailed classification of DEGs through GO analysis, as shown in Supplementary Fig. 2.

Moreover, we utilized the KEGG pathway analysis to explore the biological pathways of the target DEGs (Fig. 4A, B). In GBG vs NBG, a substantial number of genes were significantly enriched in the Parkinson's disease pathway, while in FBG vs GBG, most genes were most significantly enriched in MicroRNAs in cancer, cytokine–cytokine receptor interaction, and ABC transporters. Notably, in FBG vs NBG, DEGs were significantly enriched in Influenza A, Epstein–Barr virus

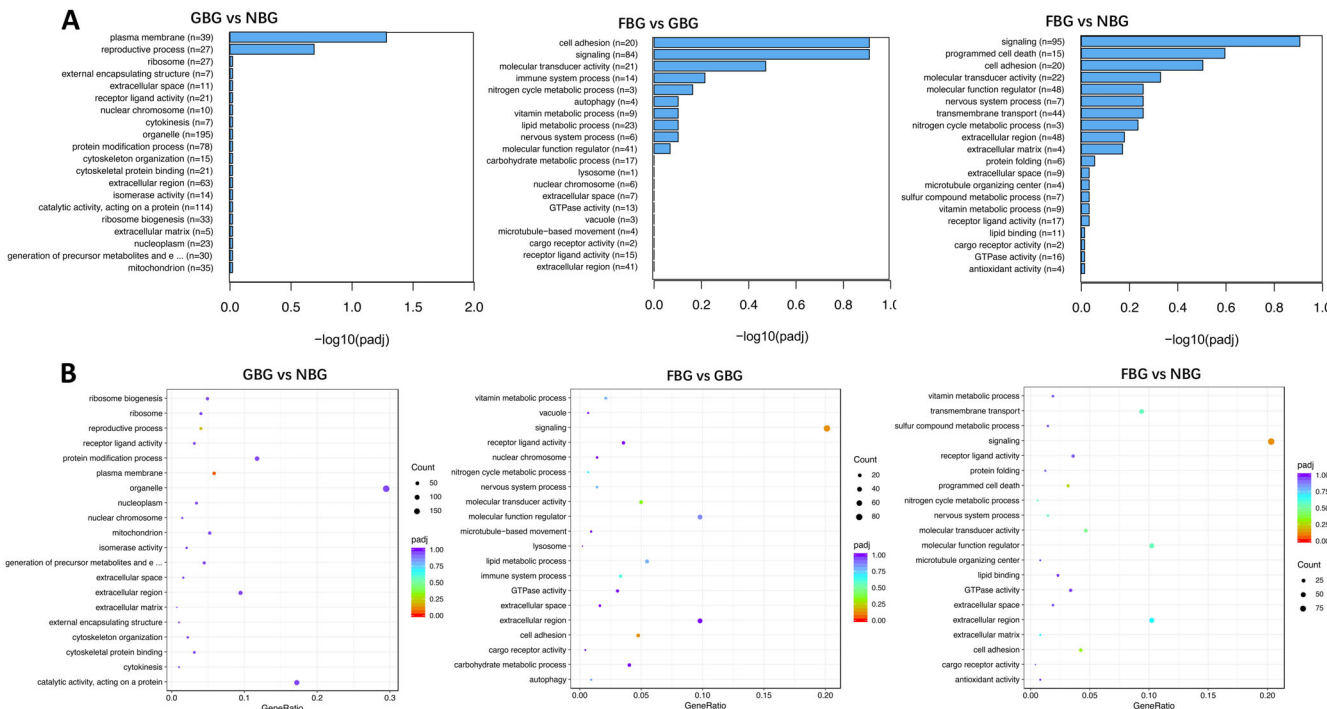


Fig. 3 | Functional annotation analysis of DEGs in different breeds of LTL in black goat breeds. A The top 20 KEGG enrichments of target DEGs compared among three different black goats; **B** Bubble diagram of the top 20 KEGG for the GBG vs NBG, FBG vs GBG, and FBG vs NBG comparisons.

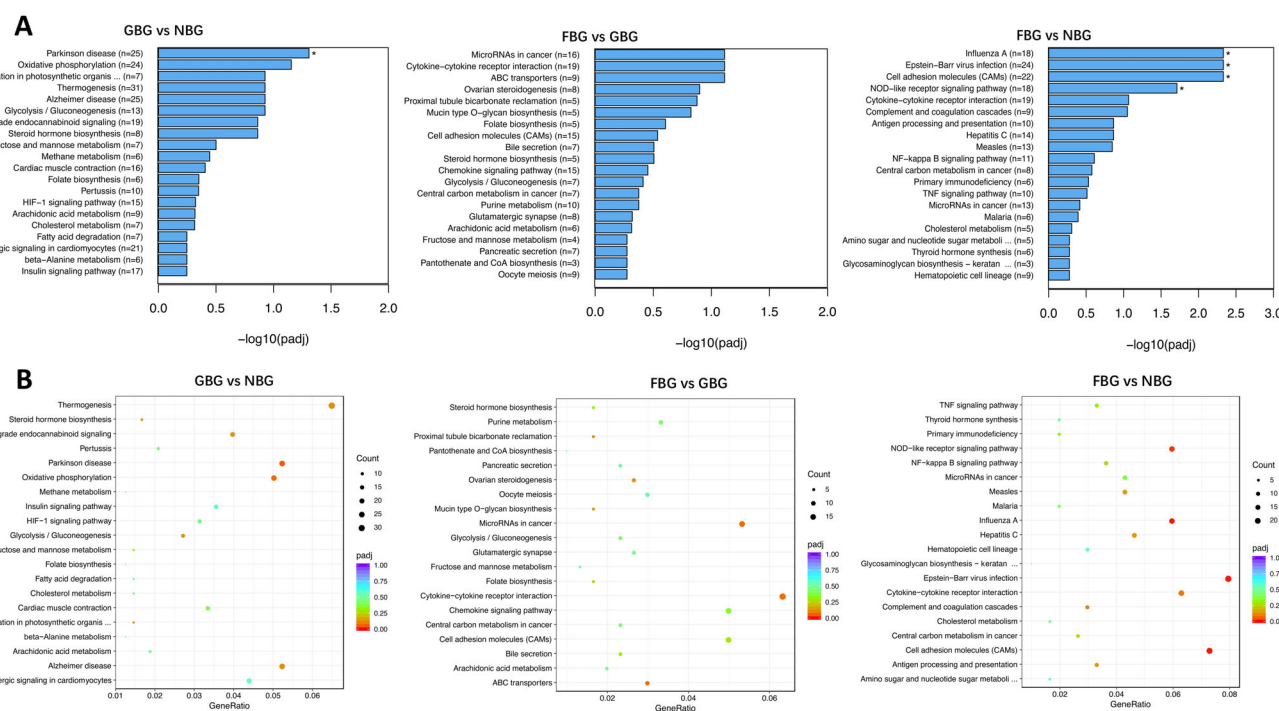


Fig. 4 | KEGG analysis of DEGs in different breeds of LTL in black goat breeds. A The top 20 KEGG enrichments of target DEGs compared among three different black goats; **B** Bubble diagram of the top 20 KEGG for the GBG vs NBG, FBG vs GBG, and FBG vs NBG comparisons; * $P < 0.05$.

infection, Cell adhesion molecules (CAMs), and NOD-like receptor signaling pathway.

Based on KEGG pathway analysis, all enriched DEGs related to IMF and IMP were selected and uploaded to the STRING website to construct the PPI network (interaction score ≥ 0.7) (Supplementary Data 4). The STRING data were exported to Cytoscape to visualize the PPI network and identify key hub genes based on color variations (Fig. 5). In the PPI

network related to IMF formation (Fig. 5A), the genes with the highest network weights included *AKT1*, *PIK3R3*, *MET*, *PFKM*, *TPI1*, *FOXO1*, *MDM2*, and *IL1B*, which may play an important role in IMF formation. In the PPI network diagram affecting IMP (Fig. 5B), we speculated that genes such as *ND4L*, *CYTB*, *COX1*, *ND2*, *NDUFB11*, *NDUFA6*, *NDUFB1*, *UQCRC*, *COX6A2*, and *GADL1* may play an important role in IMP.

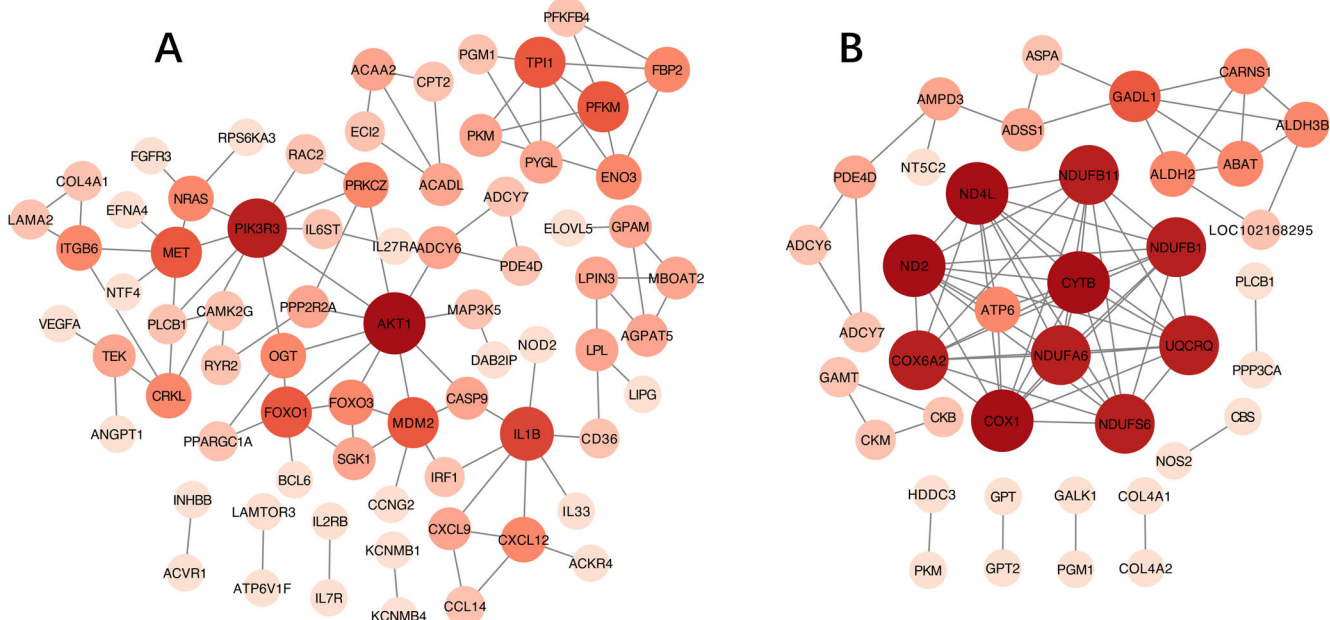
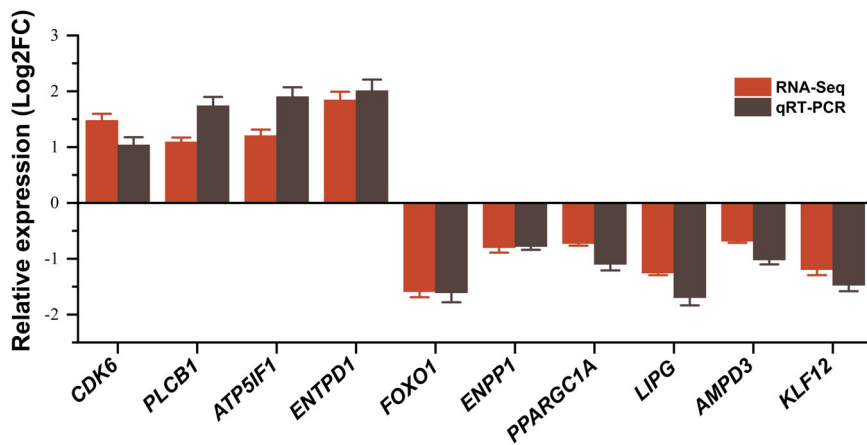


Fig. 5 | Protein-protein interaction (PPI) network analysis related to IMP and IMF and identification of their major effect genes. A Protein-protein interaction (PPI) network diagram of DEGs enriched in IMF-related pathways; **B** Protein-protein interaction (PPI) network diagram of DEGs enriched in IMP-related

pathways. The node represents DEGs and lines represent interactions between two genes. The larger the node and the darker the color, the larger the degree value in Cytoscape.

Fig. 6 | Validation of DEG-measured genes from RNA-seq using RT-qPCR, with FPKM value was used to represent the RNA-Seq result (left bar), $2^{-\Delta\Delta Ct}$ representing the RT-qPCR result (right bar).



qRT-PCR validation of DEGs in different breeds of black goats

Ten differentially expressed genes were randomly selected for qRT-PCR validation and the results are shown in Fig. 6. The analysis of relative expression levels for 10 randomly selected differentially expressed genes by qRT-PCR was consistent with the trends observed in the RNA-Seq data, indicating the reliability of the transcriptome sequencing results.

Discussion

In this study, the pH values in the three groups were higher. This is attributed to the goat's excitable nature and susceptibility to postmortem stress, which typically results in a higher pH value (5.7–6.3)⁸. Generally, the a^* value is positively correlated with meat quality, whereas the L^* and b^* values are negatively correlated with meat quality⁹. In well-bled animals, myoglobin constitutes ~90% of the total pigment in meat, while hemoglobin and cytochromes account for the remaining 10%¹⁰. However, the Fe^{2+} in myoglobin is easily oxidized to Fe^{3+} , forming yellowish-brown to gray denatured metmyoglobin, a key factor in meat color change¹¹. In this study,

compared to the GBG group, the L^* value of FBG meat after crossbreeding decreased, while the a^* value of the FBG group significantly increased compared to the NBG group. This suggests that FBG may partially inhibit the oxidation of Fe^{2+} in myoglobin to Fe^{3+} , thereby improving meat color. Moreover, we found that the tenderness and water holding capacity of the meat in the FBG group were significantly improved compared with those in the GBG group. This suggests that FBG goat meat may exhibit higher IMF deposition and improved water retention. Such meat is likely to be more tender and juicy, making it more appealing to consumers^{9,12}.

Generally, Ash content in meat is inversely related to quality; lower Ash content may indicate less inorganic matter and better meat quality¹³. In this study, the Ash content in mutton could be reduced through hybridization technology, which can further improve the quality of the meat. However, regarding the influence of mineral content on meat quality, the redox balance in the body is affected by the content of minerals such as Zn, Cu, and Fe. Compared with Fe, Zn is a moderate antioxidant and competes with Fe during absorption in the body¹⁴. Fe is a catalyst for fat oxidation, and too

high a content will reduce meat quality, particularly when it interacts with Cu, which is already a catalyst for oxidation reactions. Their interaction will aggravate lipid peroxidation and produce a large amount of reactive oxygen species (ROS)^{15–17}. To our knowledge, Zn can reduce cell membrane damage from oxidative stress by removing Cu and Fe from their binding sites on the membrane¹⁷. Additionally, Mn is a trace element with crucial physiological roles. It boosts antioxidant capacity by activating manganese superoxide dismutase (MnSOD). Interestingly, Mn also is a component of metalloenzymes like arginase, glutamine synthetase, and pyruvate carboxylase^{18,19}. In our study, compared with the GBG group, Fe in crossbred goat muscle was significantly reduced, while Zn and Cu contents remained almost unchanged. On the contrary, the Mn content in the FBG group was significantly increased.

Muscle tenderness is closely related to muscle fiber content. The number, area, and diameter of muscle fibers are negatively correlated with the tenderness of meat^{20–22}. In this study, compared with the GBG group, the muscle fiber number and total muscle fiber area in the FBG group were significantly improved. Unexpectedly, the WBSF of the FBG group was significantly lower than that of the GBG group, which appears somewhat contradictory. We speculate that this result may be due to the change in the muscle fiber type composition of FBG caused by hybridization. Specifically, hybridization may increase the proportion of type I (slow-twitch oxidative fibers) and type IIA muscle fiber (fast-twitch oxidative-glycolytic fibers) in FBG, which are positively correlated with meat tenderness^{23–25}. Regrettably, this study did not include a more detailed analysis of the composition of muscle fiber types. Of course, these current speculations will need further research and verification. Additionally, the FBG group had a significantly smaller myofiber diameter than the GBG group, which would further explain its lower WBSF.

IMF deposition largely determines fat content, and changes in IMF are closely linked to the tenderness and juiciness of mutton^{26,27}. Currently, the ideal IMF content in mutton is debated. Many researchers, such as Lambe et al.²⁸ and Pannier et al.²⁹ argued that it should range from 3.5% to 5%, while others, including Hopkins et al.³⁰ believed it should exceed 5% for better consumer preference. However, Realini et al.²⁷ investigated the consumer preference response to increasing levels of IMF mutton. They found that the consumer preference response followed a linear pattern with increasing IMF levels, with most consumers preferring mutton with higher IMF content. In this study, the IMF content and area of FBG were significantly improved, which was between GBG and NBG. As anticipated, the IMF content in all three groups was above 5%, which is strongly correlated with improvements in meat tenderness and juiciness.

In molecular biology, the glycolysis pathway is one of the important pathways regulating fat deposition³¹. When the activity of the glycolytic pathway increases, muscle cells are more inclined to obtain energy through glucose metabolism, thereby reducing their reliance on fatty acid oxidation. In this state, the availability of glucose and its conversion to acetyl-CoA inhibits the entry of fatty acids into the mitochondria as described in the glucose-fatty acid cycle (also known as the Randall cycle). The cycle emphasizes how increased glucose metabolism inhibits fatty acid oxidation, allowing for more efficient use of glucose as a primary energy source and thus reducing the conversion of glucose to the fatty acid synthesis pathway^{32–34}. Phosphofructokinase (PFK, EC 2.7.1.11), also called 6-phosphofructokinase, catalyzes the MgATP-dependent phosphorylation of fructose-6-phosphate to produce ADP and fructose-1,6-bisphosphate. It serves as the key rate-limiting enzyme in glycolysis and the primary control point for glucose metabolism³⁵. Muscle phosphofructokinase (PFKM) is a key isoform of PFK. It catalyzes the irreversible conversion of fructose-6-phosphate into fructose-1,6-bisphosphate in the glycolysis pathway and is positively correlated with elevated rates of glycolysis^{35,36}.

In this study, PFKM (log2 FC = 3.53) was significantly upregulated in GBG vs NBG, while it was significantly downregulated in FBG vs GBG (log2 FC = -2.82). Moreover, our results showed that the contents of IMF, SFA, MUFA, and UFA in the FBG group were significantly higher than those in the GBG group. We speculate that this result is due to increased

PFKM expression accelerating the glycolysis rate, causing the glucose metabolism pathway to compete with the lipogenesis pathway for energy resources. This accelerates glucose utilization and reduces the efficiency of its conversion to fatty acids, thereby decreasing fat deposition. However, when PFKM expression is reduced, glycolysis efficiency will be affected. At this time, insulin sensitivity may also be impaired, leading to insulin resistance. This impairment is largely attributable to decreased glycolytic enzyme activity in the liver and reduced glucose transport in muscle^{37,38}. The reduced glucose metabolism rate may cause unused glucose to be converted into fat for storage through pathways such as gluconeogenesis, which can indirectly promote increased fat deposition. Notably, our results showed that the insulin resistance pathway was upregulated and glycolysis/gluconeogenesis was downregulated in black goats after hybridization (Supplementary Data 3), which further supports our speculation. Additionally, interestingly, Moeller et al. demonstrated that increased glycolytic potential raises the pH, L*, and b* values in meat³⁹. However, previous studies have shown that an increase in the glycolysis rate will lead to lactic acid accumulation and a decrease in muscle pH, increasing the oxidation reaction of heme iron ($\text{Fe}^{2+} \rightarrow \text{Fe}^{3+}$), thereby reducing a* value^{40,41}. This would well explain our results that FBG obtains lower L* and higher a* values.

The *Wnt* signaling pathway is crucial in the regulation of muscle adipogenesis. The *Wnt* signaling pathway inhibits muscle adipogenesis by suppressing the expression of the CCAAT/enhancer binding proteins α (*C/EBP* α) and peroxisome proliferator-activated receptor γ (*PPARG*) genes^{42,43}. Additionally, the *Wnt* signaling pathway will inhibit adipocyte differentiation by suppressing the expression of *C/EBP* α and *PPARG*, two transcription factors essential for adipogenesis⁴⁴. Notably, the *Wnt* signal transduction primarily involves three pathways: canonical *Wnt* (*Wnt*/ β -catenin), non-canonical planar cell polarity (PCP), and non-canonical *Wnt*/ Ca^{2+} . All three pathways require binding to the transmembrane receptor frizzled (FZD) to regulate intracellular responses⁴⁵. However, *FZD4* is a key member of the frizzled family⁴⁶. When *Wnt* binds to *FZD4* and low-density lipoprotein receptor-related protein (LRP) co-receptors, it triggers an intracellular signaling cascade that promotes the stabilization and nuclear translocation of free cytoplasmic β -catenin, thereby inhibiting adipogenesis by blocking the expression of *PPAR* γ and *C/EBP* α ^{43,47}. We found that the *Wnt* pathway was significantly upregulated in GBG vs NBG. However, the *Wnt* pathway was significantly downregulated in FBG vs GBG. Importantly, we also found that the expression of *FZD4* (log2 FC = -5.2097) in the muscles of FBG compared to GBG was significantly downregulated, indicating that hybridization inhibited *FZD4* expression, subsequently downregulating the *Wnt* pathway. Finally, the deposition of IMF in goat muscles was indirectly promoted.

In this study, we identified several pathways involved in regulating IMF deposition, including the *ABC* transporter pathway, glycolysis/gluconeogenesis, *Wnt* signaling pathway, *FOXO* signaling pathway, insulin resistance, *PI3K-Akt* signaling pathway, and *PPAR* signaling pathway. Collectively, 61, 27, and 15 downregulated DEGs and 58, 50, and 67 upregulated DEGs related to IMF deposition were identified through transcriptome screening in the comparison groups GBG vs NBG, FBG vs GBG, and FBG vs NBG, respectively (Supplementary Data 4).

Typically, we pursue higher PUFA in meat because it plays a dominant role in human health and meat flavor, earning it the label of healthier meat^{48,49}. Oleic acid is the most representative fatty acid in mutton, followed by stearic and palmitic acids⁵⁰. However, C18:0 has the function of improving the flavor of meat⁵¹. Unlike previous studies, our results show that C16:0, C18:0, and C18:2 are the predominant fatty acids, particularly in the FBG group, where their levels are significantly higher than in the GBG group. As mentioned above, this phenomenon may be due to hybridization technology promoting increased IMF deposition, which results in higher SFA and MUFA content in muscle since intramuscular phospholipid content remains relatively constant and is mainly rich in PUFA, whereas the neutral lipids are mainly formed by SFA and MUFA, increase as intramuscular fat content rises⁵². However, as fat content increases, SFA and

MUFA levels rise more rapidly than PUFA production, ultimately reducing the PUFA/SFA ratio in our results⁵³.

Additionally, we believe that another key reason may be that hybridization technology has altered the composition of rumen microorganisms in goats, promoting biohydrogenation and converting more PUFA into SFA. Once this process is completed in the rumen, these fatty acids enter systemic circulation through the cells lining the small intestine and subsequently enter the bloodstream for transport to various tissues, including muscle. Therefore, they are ultimately increasing the SFA content in FBG⁵⁴⁻⁵⁶. However, under the conditions of the present study, the precise mechanism underlying this effect requires further investigation and validation. It is worth noting that a high intake of n-6 fatty acids in the human body is considered harmful and may lead to thrombosis and inflammation. Consequently, A high n-6/n-3 ratio in meat is considered pro-inflammatory and pro-thrombotic, contributing to diseases such as atherosclerosis and obesity^{57,58}. Unexpectedly, in the current study, the FBG group showed the highest n-6 content, AI index, and TI index, with no observed improvement. However, the PUFA content and the n-6/n-3 ratio among the three groups were not statistically significant. From the fatty acid profile results we obtained, it appears that the fatty acids in the muscles of the hybrid goats have not improved much, and the quality even seems to have declined. Taken together, these seemingly unexpected results make our study more interesting and mysterious, indicating that there is still a long way to go in studying hybridization to improve fatty acids in black goats.

As we all know, EAA, BCAA, and LAA are essential for animal growth and development. It is also significant that Phe plays a significant role in regulating central nervous system function^{59,60}. In this study, the EAA, BCAA, LAA, and Phe contents in the FBG group were significantly higher than in the GBG group, indicating that hybridization technology improved the key amino acid composition in black goats. Furthermore, the levels of amino acids with glucogenic, ketogenic, and glucogenic-ketogenic effects are also key factors in assessing meat quality. Glucogenic amino acids are those that can be converted into glucose through gluconeogenesis (including Ser, His, Arg, Cys, Pro, Ala, Glu, glutamine, Asp, asparagine, and Met); Ketogenic amino acids (including Leu and Lys) can be converted into ketone bodies during the process of ketogenesis, serving as alternative oxidation products of free fatty acids in the liver; glucogenic-ketogenic amino acids can produce both glucose and ketones (including Iso, Thr, Phe, Tyr, and Try)⁶¹. In this study, the Arg and Met contents among the glucogenic amino acids in the FBG group were significantly higher than in the GBG group but not statistically different from the NBG group. Similarly, the contents of Leu, Lys, and Phe in the FBG group among the ketogenic and glucogenic-ketogenic amino acids showed comparable results. Notably, the same was true for the FAA content in the FBG group. Additionally, it is important to note that amino acids are also key contributors to meat flavor, as they react with reducing sugars through the Maillard reaction to produce a variety of flavor compounds⁶². It is well known that DAA plays a key role in forming flavor compounds in meat, particularly Glu and Asp^{2,63}. In this study, the DAA content in the FBG group was significantly higher than in the GBG group, while no difference was observed between the FBG and NBG groups. In conclusion, our current data support the possibility that hybridization can improve the quality and composition of amino acids in black goat meat, as well as improve meat flavor.

After the animal is slaughtered, ATP rapidly degrades under anaerobic conditions. It is hydrolyzed into ADP by ATPase, then further broken down into AMP, and finally converted into IMP through deamination by AMP deaminase (AMPD)^{64,65}. IMP is an intermediate product of nucleotide metabolism, with an umami taste 40 times stronger than that of sodium glutamate (MSG). As a result, it is recognized as the primary umami compound in meat and plays a crucial role in enhancing its umami flavor⁶⁶. Moreover, IMP breakdown products also react with certain amino acids in Maillard reactions, producing various flavor compounds that influence meat's umami profile². However, this series of degradation processes does not stop at IMP, it will be further degraded into inosine and hypoxanthine⁶⁷. Reports indicate that hypoxanthine increases the bitterness of meat⁶⁸. In this

study, IMP levels in the NBG group were significantly higher than those in GBG, as was ADP. However, the AMP levels in each group were not statistically significant. We speculate that this may be due to the fastest ATP degradation rate in the NBG group after slaughter, resulting in the highest ADP levels. At this stage, AMPD activity in the NBG group may also have been elevated, thereby accelerating the conversion of AMP to IMP, ultimately leading to higher levels of both IMP and hypoxanthine. Unfortunately, we did not detect ATP in our study, further indicating that ATP degrades rapidly after slaughter.

In molecular biology, purine metabolism is widely recognized as a key pathway influencing IMP generation, primarily regulated positively by the AMPD, Ectonucleotide Pyrophosphatase/Phosphodiesterase (ENPP), Ectonucleoside Triphosphate Diphosphohydrolase (ENTPD), Phosphoribosyl Pyrophosphate Synthetase (PRPS) gene families^{65,66,69}. As previously mentioned, AMP is converted to IMP through the deamination activity of AMPD, an enzyme with three isoforms (AMPD1, AMPD2, and AMPD3). This highly regulated and versatile enzyme plays a key role in the adenylate catabolism pathway⁶⁵. Li et al.⁶⁹ indicated that ENPP1, a member of the ENPP family, is a type II transmembrane glycoprotein expressed in various tissues. It has dual nucleotide pyrophosphatase and phosphodiesterase activities and is involved in the hydrolysis of purine nucleotides across a range of physiological processes. ENPP1 can hydrolyze extracellular ATP to produce AMP, which subsequently participates in the purine metabolic pathway to generate IMP. Likewise, ENTPD1 is an ectonucleotidase that metabolizes ATP and ADP in the extracellular environment into AMP and phosphate⁷⁰. Notably, ENTPD8 is involved in the salvage pathway of IMP synthesis, broadly regulating multiple genes associated with IMP metabolism and promoting IMP production⁷¹. Previous studies have shown that PRPS, comprising three subtypes (PRPS1, PRPS2, and PRPS3), is a crucial enzyme for the production of Phosphoribosyl pyrophosphate (PRPP). PRPP serves as the fundamental substrate for the biosynthesis of purine and pyrimidine nucleotides and is a key precursor for IMP synthesis, playing a vital role in the purine metabolic pathway⁷²⁻⁷⁴. In this study, the purine metabolism pathway was downregulated in GBG vs NBG, including a significant downregulation in the expression of the AMPD3 gene ($\log_2 FC = -0.9172$) from the AMPD family and the RNPP1 gene ($\log_2 FC = -0.7960$) from the ENPP family. In contrast, in FBG vs GBG, the purine metabolism pathway was upregulated, with a significant upregulation of the AMPD3 gene ($\log_2 FC = 0.9172$) in the AMPD family, the ENPP1 gene ($\log_2 FC = 1.9017$) in the ENPP family, the ENTPD1 ($\log_2 FC = 1.5685$) and ENTPD8 ($\log_2 FC = 4.8374$) genes in the ENTPD family, and the PRPS2 gene ($\log_2 FC = 1.7144$) in the PRPS family. This suggests that FBG may increase the expression of related genes by upregulating the purine metabolism pathway and other pathways associated with IMP deposition in muscles, ultimately leading to greater IMP accumulation in muscle tissue.

Additionally, based on KEGG pathway analysis of the transcriptome data, we identified several pathways related to IMP deposition, including purine metabolism, the cGMP-PKG signaling pathway, alanine, aspartate, and glutamate metabolism, and the arginine biosynthesis pathway. Consequently, we identified many genes related to IMP deposition from these KEGG pathways, including 61 DEGs in GBG vs NBG (41 upregulated and 20 downregulated), 34 DEGs in FBG vs GBG (22 upregulated and 12 downregulated), and 32 DEGs in FBG vs NBG (6 upregulated and 26 downregulated). All identified genes directly or indirectly influence muscle IMP deposition (Supplementary Data 4).

In conclusion, under the conditions of this study, this study demonstrated that the meat quality of FBG (F1 hybrid of GBG and NBG), was significantly improved, with better IMF and IMP deposition, contributing to greater tenderness and flavor than GBG. Importantly, transcriptome analysis revealed a substantial number of genes associated with IMF and IMP deposition. Taken together, PFKM and FZD4 were significantly and strongly associated with IMF deposition, whereas AMPD3, ENPP1, ENTPD1, ENTPD8, and PRPS2 exhibited a significant and strong correlation with IMP deposition. This study offers important data for the future regulation of IMF and IMP deposition in GBG and breed improvement.

Nevertheless, the influence of key gene expression on the regulatory mechanisms of IMF and IMP still requires further comprehensive validation.

While this study has extensively revealed the effect of hybridization technology in significantly improving FBG meat quality, it is not without its limitations. For instance, environmental factors, genetic variation, and variations in the varieties and growth conditions of feed materials could also affect the observed traits differently. Future research and further validation are necessary. In the future, we will aim to use the confirmed target genes as molecular markers following additional verification. Additionally, by utilizing the genomic and phenotypic data of GBG, NBG, and their hybrids, we aim to construct a reference population with both phenotypic and genotypic information on meat quality traits. Through multi-generational selection, we will optimize the meat quality traits of this population over time. Finally, as a local specialty breed, GBG will be improved through the combination of marker-assisted and genomic selection programs, resulting in superior meat quality. The objective is to create a high-end mutton brand, similar to the “Guizhou black goat high-end goat meat,” to enhance regional agricultural competitiveness.

Methods

Animal ethics statement

All animal procedures strictly followed animal welfare guidelines and regulatory oversight by the Experimental Animal Ethics Committee of Guizhou University in Guizhou, China (EAE-GZU-2022-E052).

Experimental design, diet, and management

Three goat genotypes, GBG (♂), NBG (♂), and GBG (♀) × NBG (♂) crossbred F1 black goats (FBG ♂) were used. A total of 21 male goats with an initial body weight of 39.13 ± 1.65 kg were selected and divided into 3 groups (7 goats of each genotype, $n = 7$) by Completely Randomized Design. Each goat was fed a fermented total mixed ration (FTMR) as a basal diet. The experimental period spanned 90 days, comprising 15 days of adaptation followed by 75 days dedicated to data and sample collection.

The composition and nutrient levels of the total mixed ration based diet, formulated according to the NRC's⁷⁵ nutritional requirements are shown in Table 7. The FTMR production method is as follows: the mixed fermentation agent (composed of various beneficial bacteria such as *Bacillus subtilis*, yeast, lactic acid bacteria, *Bacillus licheniformis*, *Enterococcus faecalis*, and biological enzyme preparations, the number of live bacteria is $\geq 2.0 \times 10^9$ CFU/g) was purchased from Haowangnong Biotechnology Co., Ltd., Zhengzhou, China, and it was then thoroughly mixed with all the raw materials, packed into silage fermentation bags (70 cm × 130 cm × 22 cm), ferment them at room temperature for 20 days. Each goat was housed individually in a 2 m² metabolic cage. The experiment goats were fed at 9:00 and 17:00 every day on schedule.

Meat quality trait parameters

The goats were slaughtered on the last day of the experiment. Black goat was stunned by the electric shock and hung up. The jugular vein and carotid artery were cut, and the organs, forelimb knee joints and hind limb toe joints were removed. The LTL was collected to analyze the meat quality traits. The method for detecting pH, lightness (L*), redness (a*), and yellowness (b*) values in meat follows the approach outlined by Long et al.². Moreover, Samples were steamed in a preheated water bath to analyze the cooking loss according to the method of Abhijith et al.⁷⁶. The WBSF of cooked meat samples (cooked to a peak internal temperature of 71 °C) was analyzed with a TAXT2 texture analyzer (Texture Technologies Corp) with a crosshead speed of 3.5 mm/s. Each muscle sample (1 cm × 1 cm × 2 cm) was cut as parallel to the muscle fiber direction as possible in 3 replicates⁷⁷.

Sample collection, IMF content, nutritional and mineral composition, IMP and decomposition products

The petroleum ether Soxhlet extraction method for analyzing IMF content in muscle follows the approach outlined by Li et al.⁷⁸. Regarding

Table 7 | Approximate composition and nutritional levels of diet (%), air-dry basis)

Ingredient	Basal diet
Corn	56.5
Soybean meal	5.30
Yeast	3.60
NaCl	0.60
1% composite premix ^a	0.80
Soybean Oil	4.20
NaHCO ₃	0.50
Sugarcane molasses	2.00
Peanut vine	12.50
Whole-plant corn silage	14.00
Total	100.00
Chemical composition ^b	
Dry matter, DM	67.29
Neutral detergent fiber, NDF	22.41
Crude Protein, CP	13.90
Ether extract, EE	5.22
Lysine	0.63
Methionine	0.20
Methionine + Cysteine	0.37
Metabolizable Energy, ME(MJ/kg)	15.36

^aPremix provides per kg of ration: Vitamin A, 1.35×10^6 IU; Vitamin D, 4.16×10^5 IU; Vitamin E, 3000 IU; Zinc, 14.5 g; Iron, 17.0 g; Copper, 1.4 g; Manganese, 13.5 g; Iodine, 270.0 mg; Selenium, 170.0 mg; Cobalt, 40.0 mg; Ca, 12% and P, 6%.

^bExcept for lysine, methionine, methionine + cysteine, and energy value, the remaining chemical components are actual measured values.

the chemical composition of meat, the CP (Method No. 981.10) and Ash (Method No. 938.08) were analyzed according to methodologies described by the AOAC⁷⁹. Trace elements were analyzed by Inductively Coupled Plasma Mass Spectrometry (ICP-MS, 7900, Agilent, America) according to the method described by Wang et al.⁸⁰. The sample preparation method for analyzing IMP and decomposition products (hypoxanthine, inosine, AMP, and ADP) in LTL follows the approach outlined by Long et al.².

IMF and muscle fiber properties

The muscle fiber properties method followed the method outlined by Deng et al.². We utilized the PANNORAMIC panoramic slice scanner (PANNORAMIC DESK/MIDI/250/1000, 3DHISTECH, Hungary) to scan and image the muscle tissue slices. Afterward, CaseViewer2.4 scanning and browsing software (3DHISTECH, Hungary) was used to measure the number and diameter of muscle fibers in five fields of view per slice at 400x magnification. Additionally, after the muscle was stained with oil red O (ORO), the Indica Labs - Area Quantification v2.1.3 module (Indica Labs USA) in Halo v3.0.311.314 analysis software was used to quantify the area of muscle tissue in each slice, and the tissue area and IMF area were measured. IMF area was calculated using the following equation (1):

$$\text{IMF area (\%)} = \text{positive area/tissue area} \times 100\%.$$

Fatty acid profiles and amino acid profiles

A precise 1.7 g of the sample was weighed and hydrolyzed using the acid hydrolysis method. Then the fatty acid components in the sample were extracted using a chloroform-methanol solution according to the method of Tian et al.⁸¹. n-Hexane was used as an internal standard, and gas chromatography (GCMS-SQ8T, PE Company) was used to analyze 37 fatty acids of samples quantitatively.

Table 8 | The primer sequences

Primer	Primer sequences (5' to 3') ^a	NCBI accession number
FOXO1	F:GCAAGTTCATCCGTGTCAG R:ACTAGCCTTCAGCTGGTC	XM_018056686.1
CDK6	F:GTGGACCTCTGGAGCGTGG R:TGCCTGCTCATCAATGTCGTTAC	XM_018047426.1
ENPP1	F:TGCTGATGGATGGCTGAAGGAG R:GGTAAGGTCTGAAGTGTGGTTTG	XM_018053516.1
PLCB1	F:GGTGGTTCTCCCTCGCT R:AGGCTGGTCCCTCGT	XM_018056909.1
LIPG	F:TTGGCTTGAGCATGGCATT R:TGCGATGGTCCATATGCGATC	XM_005697191.3
PPARGC1A	F:AATGCAGTGGCCTCAGTACC R:CTGCTGTTCCGGTCTCTGT	XM_018049155.1
AMPD3	F:AGAAGAGTCCGGTGTGCAG R:CACACTGTTCCGGCATCT	XM_018059533.1
ATP5IF	F:GGAAAAAGAGAGCAGGCCGA R:GATCGACTGCTTATGCCGCT	XM_018056878.1
KLF12	F:TCTAAGGTACATTTGCAGGT R:CCAATCGGTGCCTGTTGCTAC	XM_018056508.1
ENTPD1	F:GGGACTTCAGGGTACAATGGA R:GAGCACTGGAGTAAGGGCAAT	XM_005698264.3
β -actin	F:AGATGGATCAGCAAGCAG R:CCAATCTCATCTGTTCTG	XM_018039831.1

^aF forward, R reverse.

100 mg of muscle sample was accurately weighed into a 20 ml glass hydrolysis tube and the sample was hydrolyzed by acid hydrolysis. The method for detecting the amino acid composition of the extracted sample follows the approach outlined by Long et al.², and the content of each amino acid was analyzed by an amino acid analyzer (L-8900, Hitachi, Tokyo, Japan).

RNA extraction, gene library construction and qRT-PCR verification of differentially expressed genes

RNA extraction, cDNA reverse transcription, and Quantitative PCR (qRT-PCR) were performed according to the method described by Long et al.². Briefly, total RNA was extracted from the LTL of black goats using the Trizol method. The integrity and concentration of the extracted RNA were evaluated using a NanoDrop One 2000 spectrophotometer (Thermo Scientific, Waltham, MA, USA). Subsequently, cDNA synthesis was performed with the cDNA Reverse Transcription Kit (Beijing Kangwei Century Biotechnology Co., Beijing, China). The reverse transcription reaction was conducted in a total volume, including 1 μ L of HiFiScript (200 U/ μ L), 1 μ L of Primer Mix, and 4 μ L of 5 \times ScriptRT Buffer, with RNase-free water added to reach the final volume of 20 μ L. The reaction conditions were set as follows: incubation at 42 °C for 15 min, followed by 85 °C for 5 min. The synthesized cDNA was then stored at -20 °C for subsequent analyses. qRT-PCR reactions were performed in triplicate for each sample type/primer set combination. The expression level of each gene relative to GAPDH was evaluated using the $2^{-\Delta\Delta Ct}$ method described by Livak and Schmittgen⁸². The gene series used to verify the reliability of transcriptomic sequencing are shown in Table 8.

Transcriptome sequencing

The de novo transcriptome sequencing for this study was completed by Beijing Novogene Technology Co., Ltd. The image data converted from the sequencing fragments are converted into sequence data (reads) after Illumina Casava (v1.8) software base recognition. To ensure the quality and reliability of subsequent data analysis, Trinity software (v2.6.6) was used to assemble clean reads into transcript sequences, and then BUSCO software (v3.0.2) was used to evaluate the accuracy and completeness of the assembly

results. Finally, the alignment RSEM software (v1.3.3) was used to map the clean reads of each sample to the reference sequence, filter out unqualified reads, and obtain the read counts mapped to each gene. After the evaluation was qualified, clean reads for subsequent analysis could be obtained.

To control the proportion of false positives, the P_{adj} value was introduced to correct the P value. The expression levels of differentially expressed genes between GBG vs NBG, FBG vs GBG, and FBG vs NBG were analyzed by DESeq 2 software (v1.26.0). We have grouped the samples in advance and calculated the Fold Change value based on the average read counts. Next, we used $|Fold\ Change| \geq 0$ and $p\ value < 0.05$ as the DEGs screening criteria to evaluate whether there is a significant difference in gene expression between groups.

To clarify the biological functions in which differentially expressed genes are involved, we used GOSeq (v1.32.0) and topGO (v2.32.0) software to analyze gene functions at three levels according to the Gene Ontology (GO) database (<http://www.geneontology.org/>): BP, CC, and MF⁸³. The top 20 most significant terms are selected to draw a histogram. The threshold for significant enrichment was set at $p_{adj} < 0.05$.

Furthermore, to clarify the main metabolic and signaling pathways involving the differentially expressed genes, we used the Kyoto Encyclopedia of Genes and Genomes (KEGG, <http://www.genome.jp/kegg/pathway.html>)⁸⁴ method for elaboration. KOBAS software (v3.0) was used to find pathways with significantly enriched differential genes. The threshold for significant enrichment was set at $p_{adj} < 0.05$. Notably, in this study, all transcriptome-related data analyses, including DEG screening and the generation of all graphics, were performed using the cloud tool option in the NovoMagic platform system (<https://magic.novogene.com/>) independently developed by Novogene Co., Ltd.

Statistical analysis

All raw data were compiled using Excel 2022 and statistically analyzed using SPSS 23.0 software. First, the Shapiro-Wilk test was used to determine the normal distribution of all raw data. Next, all raw data that met normal distribution were subjected to one-way ANOVA and the general linear model (GLM module) of multivariate ANOVA. Finally, we used the LSD method and Duncan test for multiple comparisons and significant difference testing. The table in the text shows the mean and standard error (SEM) of each group. $P < 0.05$ was considered significant and $P < 0.01$ was considered extremely significant, and the degree of significance can be obtained based on the specific P value in the table.

Data availability

The sequencing data of this study are deposited in the NCBI repository, accession number PRJNA 1178003. Other data used to support the results of this study can be provided at the request of the corresponding author.

Received: 28 December 2024; Accepted: 6 June 2025;

Published online: 07 July 2025

References

1. Makina, S. O. et al. Extent of linkage disequilibrium and effective population size in four South African Sanga cattle breeds. *Front. Genet.* **6**, 337 (2015).
2. Long, Y. et al. Effect of mulberry leaf TMR on growth performance, meat quality and expression of meat quality master genes (ADSL, H-FABP) in crossbred black goats. *Foods* **11**, 4032 (2022).
3. Long, Y. et al. Effects of *Flammulina velutipes* mushroom residues on growth performance, apparent digestibility, serum biochemical indicators, rumen fermentation and microbial of Guizhou black goat. *Front. Microbiol.* **15**, 1347853 (2024).
4. Chang, L. et al. Identification of genomic characteristics and selective signals in Guizhou black goat. *BMC Genom.* **25**, 164 (2024).
5. Tan, X. S. et al. Establishment of regression model between body weight and body size of Guizhou black goats. *Guizhou J. Anim. Husb. Vet. Med.* **47**, 17–19 (2023).

6. Zhou, A. M. et al. Body mass index and growth model prediction analysis of Beichuan white goat and their hybrids. *J. Yunnan Agric. Univ.* **37**, 97–104 (2022).
7. Min, Y. et al. Comparison of production performance and meat quality characteristics between Guizhou Black goats and F4 generation hybrids of South African Kalaha Goats. *Sci. Rep.* **14**, 18608 (2024).
8. Gawat, M., Kaur, L., Singh, J. & Boland, M. Physicochemical and quality characteristics of New Zealand goat meat and its ultrastructural features. *Food Res. Int.* **161**, 111736 (2022).
9. Ruedt, C., Gibis, M. & Weiss, J. Meat color and iridescence: origin, analysis, and approaches to modulation. *Compr. Rev. Food Sci. F.* **22**, 3366–3394 (2023).
10. Matarneh, S. K., England, E. M., Scheffler, T. L., Gerrard, D. E. & Toldra, F. Lawrie's meat science. The conversion of muscle to meat. *Woodhead Publishing*. 159–185 (2017).
11. Zhang, L. et al. In situ growth of g-C3N4 on hexangular flowerlike FeWO4 microcrystals: highly efficient catalyst and the crucial roles of Fe3+/Fe2+ couple in the photoassisted oxidation and reduction reactions. *J. Phys. Chem. C.* **122**, 12900–12912 (2018).
12. Brand, T. S., Van Der Merwe, D. A., Hoffman, L. C. & Geldenhuys, G. The effect of dietary energy content on quality characteristics of Boer goat meat. *Meat sci.* **139**, 74–81 (2018).
13. Abdullah, A. Y. & Qadesieh, R. I. Effect of slaughter weight and aging time on the quality of meat from Awassi ram lambs. *Meat Sci.* **82**, 309–316 (2009).
14. Olivares, M., Pizarro, F., Gaitán, D. & Ruz, M. Acute inhibition of iron absorption by zinc. *Nutr. Res.* **27**, 279–282 (2007).
15. Marreiro, D. dN. et al. Zinc and oxidative stress: current mechanisms. *Antioxidants* **6**, 24 (2017).
16. Tang, L., Zhang, Y., Qian, Z. & SHEN, X. The mechanism of Fe2+ –initiated lipid peroxidation in liposomes: the dual function of ferrous ions, the roles of the pre-existing lipid peroxides and the lipid peroxy radical. *Biochem. J.* **352**, 27–36 (2000).
17. Wołonciej, M., Milewska, E. & Roszkowska-Jakimiec, W. Trace elements as an activator of antioxidant enzymes. *Adv. Hyg. Exp. Med.* **70**, 1483–1498 (2016).
18. Goluch, Z. & Haraf, G. Goose meat as a source of dietary manganese –a systematic review. *Animals* **13**, 840 (2023).
19. Li, L. & Yang, X. The essential element manganese, oxidative stress, and metabolic diseases: links and interactions. *Oxid. Med. Cell Longev.* **2018**, 7580707 (2018).
20. Matarneh, S. K., Silva, S. L. & Gerrard, D. E. New insights in muscle biology that alter meat quality. *Annu. Rev. Anim. Biosci.* **9**, 355–377 (2021).
21. Xue, J. et al. Potential mechanism and effects of different selenium sources and different effective microorganism supplementation levels on growth performance, meat quality, and muscle fiber characteristics of three-yellow chickens. *Front. Nutr.* **9**, 869540 (2022).
22. Utari, A., Warly, L., Hermon, Suyitman & Evitayani Metabolic response and meat quality of goats fed Artocarpus heterophyllus and Moringa oleifera. *Int. J. Vet. Sci.* **12**, 498–503 (2023).
23. Li, J. et al. Effect of dietary resveratrol supplementation on muscle fiber types and meat quality in beef cattle. *Meat Sci.* **194**, 108986 (2022).
24. Joo, S., Kim, G., Hwang, Y. & Ryu, Y. Control of fresh meat quality through manipulation of muscle fiber characteristics. *Meat Sci.* **95**, 828–836 (2013).
25. Cheng, H. et al. Comparison of beef quality influenced by freeze-thawing among different beef cuts having different muscle fiber characteristics. *Meat Sci.* **169**, 108206 (2020).
26. Li, L. et al. Expression patterns of peroxisome proliferator-activated receptor gamma 1 versus gamma 2, and their association with intramuscular fat in goat tissues. *Gene* **528**, 195–200 (2013).
27. Qi, H. et al. Effect of Dietary Glycerol Addition on Growth Performance, Serum Biochemical Indexes, Carcass Traits, Fat Deposition, and Meat Quality in Fattening Period Kazakh Sheep. *Kafkas Univ. Vet. Fak. Derg.* **30**, 275–282 (2024).
28. Lambe, N. et al. Prediction of intramuscular fat content using CT scanning of packaged lamb cuts and relationships with meat eating quality. *Meat Sci.* **123**, 112–119 (2017).
29. Pannier, L. et al. Intramuscular fat in the longissimus muscle is reduced in lambs from sires selected for leanness. *Meat Sci.* **96**, 1068–1075 (2014).
30. Hopkins, D., Hegarty, R., Walker, P. & Pethick, D. W. Relationship between animal age, intramuscular fat, cooking loss, pH, shear force and eating quality of aged meat from sheep. *Aust. J. Exp. Ag.* **46**, 879–884 (2006).
31. Fontanesi, L. et al. Investigation of candidate genes for glycolytic potential of porcine skeletal muscle: Association with meat quality and production traits in Italian Large White pigs. *Meat Sci.* **80**, 780–787 (2008).
32. Mazibuko-Mbeje, S. E., Dladla, P. V., Nkambule, B. B., Obonye, N. & Louw, J. The role of glucose and fatty acid metabolism in the development of insulin resistance in skeletal muscle. *Muscle Cell and Tissue-current Status of Research Field* <https://doi.org/10.5772/intechopen.75904> (2018).
33. De Mauverger, E. R. The glucose-fatty acid cycle: an old concept that never goes out of fashion. *J. ISSN* **2766**, 2276 (2024).
34. Frayn, K. The glucose–fatty acid cycle: a physiological perspective. *Biochem. Soc. Trans.* **31**, 1115–1119 (2003).
35. Wang, J. et al. Molecular characterization, expression profile, and association study with meat quality traits of porcine PFKM gene. *Appl. Biochem. Biotech.* **173**, 1640–1651 (2014).
36. Sola-Penna, M., Da Silva, D., Coelho, W. S., Marinho-Carvalho, M. M. & Zancan, P. Regulation of mammalian muscle type 6-phosphofructo-1-kinase and its implication for the control of the metabolism. *IUBMB Life* **62**, 791–796 (2010).
37. Yu, C. et al. Mechanism by which fatty acids inhibit insulin activation of insulin receptor substrate-1 (IRS-1)-associated phosphatidylinositol 3-kinase activity in muscle. *J. Biol. Chem.* **277**, 50230–50236 (2002).
38. Wu, C., Okar, D. A., Newgard, C. B. & Lange, A. J. Increasing fructose 2, 6-bisphosphate overcomes hepatic insulin resistance of type 2 diabetes. *Am. J. Physiol. Endocrinol. Metab.* **282**, E38–E45 (2002).
39. Moeller, S. J., Baas, T., Leeds, T., Emmett, R. & Irvin, K. Rendement Napole gene effects and a comparison of glycolytic potential and DNA genotyping for classification of Rendement Napole status in Hampshire-sired pigs. *J. Anim. Sci.* **81**, 402–410 (2003).
40. Møller, J. K. & Skibsted, L. H. Myoglobins: the link between discoloration and lipid oxidation in muscle and meat. *Quim. Nova* **29**, 1270–1278 (2006).
41. Mancini, R. & Hunt, M. Current research in meat color. *Meat Sci.* **71**, 100–121 (2005).
42. Christodoulides, C., Lagathu, C., Sethi, J. K. & Vidal-Puig, A. Adipogenesis and WNT signalling. *Trends Endocrinol. Metab.* **20**, 16–24 (2009).
43. Chen, X. et al. The effect of arginine on the Wnt/β-catenin signalling pathway during porcine intramuscular preadipocyte differentiation. *Food Funct.* **8**, 381–386 (2017).
44. Ross, S. E. et al. Inhibition of adipogenesis by Wnt signaling. *Science* **289**, 950–953 (2000).
45. Pan, C. et al. Genome-wide identification and expression profiling analysis of Wnt family genes affecting adipocyte differentiation in cattle. *Sci. Rep.* **12**, 489 (2022).
46. Huang, H.-C. & Klein, P. S. The Frizzled family: receptors for multiple signal transduction pathways. *Genome Biol.* **5**, 1 (2004).

47. Bagchi, D. P. et al. Wntless regulates lipogenic gene expression in adipocytes and protects against diet-induced metabolic dysfunction. *Mol. Metab.* **39**, 100992 (2020).

48. Wood, J. et al. Effects of fatty acids on meat quality: a review. *Meat Sci.* **66**, 21–32 (2004).

49. Chikwanha, O. C., Vahmani, P., Muchenje, V., Dugan, M. E. & Mapiye, C. Nutritional enhancement of sheep meat fatty acid profile for human health and wellbeing. *Food Res. Int.* **104**, 25–38 (2018).

50. Diogénes, L. V. et al. Physicochemical composition and fatty acid profile of goat kids' meat fed ground-corn-grain silage rehydrated with different additives. *Animals* **13**, 31 (2022).

51. Brennand, C. & Lindsay, R. Distribution of volatile branched-chain fatty acids in various lamb tissues. *Meat Sci.* **31**, 411–421 (1992).

52. Sharma, N., Ganderer, G. & Goutefongea, R. Comparative lipid composition of porcine muscles at different anatomical locations. *Meat Sci.* **19**, 121–128 (1987).

53. Raes, K., De Smet, S. & Demeyer, D. Effect of dietary fatty acids on incorporation of long chain polyunsaturated fatty acids and conjugated linoleic acid in lamb, beef and pork meat: a review. *Anim. Feed. Sci. Tech.* **113**, 199–221 (2004).

54. Andrade, J. C. et al. Production of conjugated linoleic acid by food-grade bacteria: A review. *Int. J. Dairy. Technol.* **65**, 467–481 (2012).

55. Badawy, S. et al. Conjugated linoleic acid (CLA) as a functional food: is it beneficial or not? *Food Res. Int.* **113158** <https://doi.org/10.1016/j.foodres.2023.113158> (2023).

56. Jenkins, T., Wallace, R., Moate, P. & Mosley, E. Board-invited review: recent advances in biohydrogenation of unsaturated fatty acids within the rumen microbial ecosystem. *J. Anim. Sci.* **86**, 397–412 (2008).

57. Taboada, N. et al. Administration of selected probiotic mixture improves body weight gain and meat fatty acid composition of creole goats. *Food Biosci.* **49**, 101836 (2022).

58. Simopoulos, A. P. An increase in the omega-6/omega-3 fatty acid ratio increases the risk for obesity. *Nutrients* **8**, 128 (2016).

59. Brzostowski, H., Niżnikowski, R. & Tański, Z. Quality of goat meat from purebred French Alpine kids and Boer crossbreeds. *Arch. Anim. Breed.* **51**, 381–388 (2008).

60. Vahmani, P. et al. Bioactivity and health effects of ruminant meat lipids. Invited Review. *Meat Sci.* **165**, 108114 (2020).

61. Migdał, W., Kawęcka, A., Sikora, J. & Migdał, Ł. Meat quality of the native Carpathian goat breed in comparison with the Saanen breed. *Animals* **11**, 2220 (2021).

62. Ramalingam, V., Song, Z. & Hwang, I. The potential role of secondary metabolites in modulating the flavor and taste of the meat. *Food Res. Int.* **122**, 174–182 (2019).

63. Tang, S. et al. Substitution of ramie (*Boehmeria nivea*) for alfalfa in improving the carcass and meat quality of Liuyang Black goats. *Anim. Nutr.* **7**, 688–694 (2021).

64. Indriani, S., Srisakultiew, N., Sangsawad, P., Paengkoum, P. & Pongsetkul, J. Characterization of the non-volatiles and volatiles in correlation with flavor development of cooked goat meat as affected by different cooking methods. *Food Sci. Anim. Resour.* **44**, 662 (2024).

65. He, L. et al. Molecular characterization of adenosine monophosphate deaminase 1 and the correlation analysis between its mRNA expression levels and inosine monophosphate content in large yellow croaker (*Larimichthys crocea*). *Comp. Biochem. Physiol. Part B Biochem. Mol. Biol.* **272**, 110966 (2024).

66. Huang, Z. et al. Analysis of the molecular mechanism of inosine monophosphate deposition in Jingyuan chicken muscles using a proteomic approach. *Poult. Sci.* **101**, 101741 (2022).

67. Mora, L., Hernández-Cázares, A. S., Aristoy, M.-C. & Toldrá, F. Hydrophilic interaction chromatographic determination of adenosine triphosphate and its metabolites. *Food Chem.* **123**, 1282–1288 (2010).

68. Utama, D. T. et al. Effects of high-pressure processing on taste-related ATP breakdown compounds and aroma volatiles in grass-fed beef during vacuum aging. *Asian-Australas. J. Anim. Sci.* **31**, 1336 (2018).

69. Li, S. et al. Cardiomyocytes disrupt pyrimidine biosynthesis in nonmyocytes to regulate heart repair. *J. Clin. Investig.* **132** <https://doi.org/10.1172/JCI149711> (2022).

70. Ehlers, L. et al. Surface AMP deaminase 2 as a novel regulator modifying extracellular adenine nucleotide metabolism. *FASEB J.* **35** <https://doi.org/10.1169/refubium-36825> (2021).

71. Ma, T. et al. Mining the key regulatory genes of chicken inosine 5'-monophosphate metabolism based on time series microarray data. *J. Anim. Sci. Biotechnol.* **6**, 1–11 (2015).

72. Qian, X. et al. Conversion of PRPS hexamer to monomer by AMPK-mediated phosphorylation inhibits nucleotide synthesis in response to energy stress. *Cancer Discov.* **8**, 94–107 (2018).

73. Maharjan, A., Singhvi, M. & Kim, B. S. Biosynthesis of a therapeutically important nicotinamide mononucleotide through a phosphoribosyl pyrophosphate synthetase 1 and 2 engineered strain of *Escherichia coli*. *ACS Synth. Biol.* **10**, 3055–3065 (2021).

74. Li, J. et al. Mechanosensitive turnover of phosphoribosyl pyrophosphate synthetases regulates nucleotide metabolism. *Cell Death Differ.* **29**, 206–217 (2022).

75. NRC (National Research Council). *Nutrient Requirements of Small Ruminants, Sheep, Goats, Cervids, and New World Camelids* 3rd edn (National Academy Press, 2007).

76. Abhijith, A. et al. Effect of slaughter age and post-mortem days on meat quality of longissimus and semimembranosus muscles of Boer goats. *Meat Sci.* **175**, 108466 (2021).

77. Han, Y. et al. Soybean oil and probiotics improve meat quality, conjugated linoleic acid concentration, and nutritional quality indicators of goats. *J. Food Sci.* **90**, e17669 (2025).

78. Li, B. et al. Identification of candidate circular RNAs underlying intramuscular fat content in the donkey. *Front. Genet.* **11**, 587559 (2020).

79. AOAC. *Official Methods of Analysis* 18th edn (Association of Official Analytical Chemist: Gaithersburg, 2005).

80. Wang, Q. et al. Discrimination of mutton from different sources (regions, feeding patterns and species) by mineral elements in Inner Mongolia, China. *Meat Sci.* **174**, 108415 (2021).

81. Tian, X., Lu, Q., Paengkoum, P. & Paengkoum, S. Effect of purple corn pigment on change of anthocyanin composition and unsaturated fatty acids during milk storage. *J. Dairy. Sci.* **103**, 7808–7812 (2020).

82. Livak, K. J. & Schmittgen, T. D. Analysis of relative gene expression data using real-time quantitative PCR and the $2^{-\Delta\Delta CT}$ method. *Methods* **25**, 402–408 (2001).

83. Young, M. D., Wakefield, M. J., Smyth, G. K. & Oshlack, A. Gene ontology analysis for RNA-seq: accounting for selection bias. *Genome Biol.* **11**, 1–12 (2010).

84. Kanehisa, M. et al. KEGG for linking genomes to life and the environment. *Nucleic Acids Res.* **36**, D480–D484 (2007).

Acknowledgements

The author(s) declare that financial support was received for the research, authorship, and/or publication of this article. This research was mainly supported by Major Special Projects of the Guizhou Province Department of Science and Technology (Qianke Service Enterprise [2020]4009). Moreover, Yong Long gratefully recognizes the Suranaree University of Technology scholarship for External Grants and Scholarships for Graduate Students (SUT-OROG 82/2566) as a source of funding.

Author contributions

Yong Long wrote the main manuscript text, subsequently revised it, and carried out the data analysis. Naifeng Zhang, Yanliang Bi, Tao Ma, Pramote Paengkoum, Wen Xiao, and Yanpin Zhao were responsible for organizing

the data, conducting transcriptome analysis, and reviewing and revising the manuscript. Chao Yuan, Defeng Wang, Yang Yang, and Chanzhi Su executed the experiment, which involved animal husbandry, sample collection, and analysis. Yong Han provided overall supervision, managed the experiment, reviewed the manuscript, verified the data, and coordinated the project.

Competing interests

The authors declare no competing interests.

Additional information

Supplementary information The online version contains supplementary material available at <https://doi.org/10.1038/s41538-025-00476-x>.

Correspondence and requests for materials should be addressed to Yong Han.

Reprints and permissions information is available at <http://www.nature.com/reprints>

Publisher's note Springer Nature remains neutral with regard to jurisdictional claims in published maps and institutional affiliations.

Open Access This article is licensed under a Creative Commons Attribution-NonCommercial-NoDerivatives 4.0 International License, which permits any non-commercial use, sharing, distribution and reproduction in any medium or format, as long as you give appropriate credit to the original author(s) and the source, provide a link to the Creative Commons licence, and indicate if you modified the licensed material. You do not have permission under this licence to share adapted material derived from this article or parts of it. The images or other third party material in this article are included in the article's Creative Commons licence, unless indicated otherwise in a credit line to the material. If material is not included in the article's Creative Commons licence and your intended use is not permitted by statutory regulation or exceeds the permitted use, you will need to obtain permission directly from the copyright holder. To view a copy of this licence, visit <http://creativecommons.org/licenses/by-nc-nd/4.0/>.

© The Author(s) 2025